

Raman study of Ga_{1-x}Al_xN solid solutions

F. Demangeot, J. Groenen, J. Frandon, M. A. Renucci
Laboratoire de Physique des Solides de Toulouse, Université Paul Sabatier

Olivier Briot, S. Ruffenach-Clur, Roger-Louis Aulombard
Groupe d'Etude des Semiconducteurs, GES-CNRS

This article was received on July 18, 1997 and accepted on September 17, 1997.

Abstract

Long wavelength optical phonons of Al_xGa_{1-x}N solid solutions have been identified in the whole compositional range by Raman spectroscopy. The frequencies of A₁ and E₁ polar phonons increase continuously with x from one-member crystal to the other. A generalization of the dielectric model of Hon and Faust is used to treat the coupling of the longitudinal optic (LO) mode. This approach accounts for the observed frequencies and confirms the so-called one-mode behaviour of polar LO phonons. Moreover, a signature of the coupling of a discrete mode (tentatively associated to silent q=0 B₁ mode) with an unidentified continuum has been obtained.

1. Introduction

Gallium-aluminium nitride alloys may be promising materials for optical applications, particularly for light emission in the ultraviolet range. Indeed, the forbidden band of these wide gap semiconductor alloys seems to be suitable to many applications in this spectral range. Moreover, the residual deformation in these layers, due to the lattice mismatch with the substrate (generally sapphire), may be changed by the aluminium content of the alloy.

Basic studies on these ternary solid solutions were recently developed. The literature concerning Raman spectra from Ga_{1-x}Al_xN crystals is poor: we note only the paper published by Hayashi et al. [1], who found a one-mode behaviour for the polar phonons in a very small compositional range (x ≤ 0.15). In this communication, we present a report on the dynamical properties of Ga_{1-x}Al_xN crystals (0 < x ≤ 1) investigated by Raman spectroscopy with a special attention to the behaviour of long wavelength polar phonons.

2. Samples and experiments

Eight Ga_{1-x}Al_xN layers (with 0.16 ≤ x ≤ 0.84), together with GaN layers, have been used for the present study. The 2 μm thick samples were grown by MOVPE on thin AlN buffer layers previously deposited on a (0001) sapphire substrate; the aluminium content x of the layers was determined from a measurement of the lattice constant [2]. Several AlN layers (x = 1) were also available. Unfortunately, they did not yield any useful results.

All the spectra have been recorded at room temperature in a backscattering geometry, along or perpendicular to the **c**-axis of the wurtzite crystal. Micro-Raman measurements with a lateral resolution of about 1 μm, allowing incidence on the layer edge, were performed using a Dilor set-up. The light source was the 488 nm line of a Ar⁺ laser.

3. Experimental results

Examples of Raman spectra, recorded in $x'(y'y')\bar{x}'$ and $x'(zz)\bar{x}'$ configurations, are given in Figure 1a and Figure 1b respectively (x' and y' represent two orthogonal axes perpendicular to the c axis). For low aluminium content, sharp phonon lines are clearly evidenced and most of them obey the selection rules for backscattering geometry in wurtzite crystals, as evidenced in Figure 2, for $x = 0.45$ solid solution. So the vibrational modes can be unambiguously followed in this range. However, it should be pointed out that the $E_1(\text{LO})$ phonon is found in forbidden configuration, as it was also observed for pure GaN layers. An additional weak structure peaks in the intermediate range between TO and LO phonons, around 640 cm^{-1} , on the high frequency side of the line corresponding to the E_2 phonon.

For $x > 0.5$, the intensity of Raman spectra decreases and the peaks become broader and broader. Moreover, we observe for $x > 0.7$ a complete relaxation of selection rules, probably due to the polycrystalline structure of the layers, rendering the assignment of the experimental features difficult. In spite of the lack of unambiguous signature in the whole range of composition, a plot of the measured phonon frequencies in the whole composition range is reported in Figure 3. For the extrapolation up to $x = 1$, we used the experimental phonon frequencies in AlN crystals from McNeil et al. [3], which can be compared to the values recently calculated by Karch et al. [4].

Our frequency variation is in good agreement with previous results obtained in a narrower compositional range by Hayashi et al. [1]. The continuous evolution observed in Figure 3 seems to be very satisfactory. Note the crossing of the $E_1(\text{TO})$ and E_2 modes, which is clearly found at $x = 0.35$. In spite of its uncertain signature, the wide feature evidenced near 660 cm^{-1} for high aluminium content was assigned to an E_2 mode, because it is very close to the corresponding mode in AlN [3]. Our data seem to support one-mode behaviour for the LO and TO vibration modes. On the contrary, our results concerning the E_2 phonon are quite ambiguous: weak and wide features (which did not clearly obey the usual selection rules) in the spectra might suggest a possible two mode behaviour.

The best fit of our data gives these analytical formulae for the dependence of the $A_1(\text{LO})$ and $A_1(\text{TO})$ peaks position on Al content, valid in the case where $x > 0.05$:

$$\omega_{A_1(\text{LO})} = 746 + 169.5 x + 11.7 x^2 - 36.6 x^3 \quad (1)$$

$$\omega_{A_1(\text{TO})} = 540 + 19.7 x + 31.7 x^2 + 22.2 x^3 \quad (2)$$

Phonon frequencies values are given in cm^{-1} .

Concerning the measured phonon frequencies, the experimental uncertainty is 1 or 2 cm^{-1} up to $x = 0.55$. For $x > 0.55$, this value increases up to 10 cm^{-1} .

In the Raman spectra of the solid solutions, a weak dip was observed (see Figure 1) for the whole range of composition, for parallel polarizations of incident and scattered light. Its origin seems to be related to the alloy and not to any crystalline defect, because its frequency is increasing linearly with the aluminum content (see Figure 3). This feature suggests an interference between a discrete mode and a continuum of excitations.

The discrete excitation coupled to the hypothetical continuum might be the "silent" B_1 mode in the ternary solid solutions, according to a linear frequency variation between the phonon frequencies of the pure binary compounds, calculated in ref. [4] and [5]. Activation of the silent mode in Raman spectra might proceed from a q -dependent process likely to occur in the alloys because of the breakdown of translational symmetry.

4. Presentation of the model

The purpose of the following model [6] is to calculate the frequency and the intensity of the LO $q = 0$ polar phonons in the wurtzite $\text{Ga}_{1-x}\text{Al}_x\text{N}$ solid solutions, as a function of the aluminium content. It should be noted that the non-polar E_2 modes cannot be calculated in the frame of this model.

In the calculation of coupled vibration modes in ternary solid solutions, the first step is the estimation of impurity mode frequencies. The later is usually estimated from the average frequency for $\mathbf{q}=0$ optical phonons and from its frequency shift, incoming from the extensive or compressive strain suffered by the impurity cluster in the host matrix [7]. In the present case, the phonon dispersion, as calculated by Karch et al. [4] for AlN and by Azuhata et al. [5] for GaN, was taken into account in the estimation of impurity modes, to obtain better agreement with experimental results. Due to the concavity of the LO branches at the centre of Brillouin zone, both impurity modes were shifted towards lower frequencies: we have obtained 600 cm^{-1} and 655 cm^{-1} , respectively, for Ga in AlN and for Al in GaN (instead of the values 631 cm^{-1} and 684 cm^{-1} , when only $\mathbf{q}=0$ optical phonons are taken into account).

The second step is to define the “mechanical» frequencies $\omega_{T_i}(x)$, for each uncoupled oscillator ($i=1$ or 2 , for AlN or GaN respectively) in the solid solution, as a function of x : a linear variation of these frequencies will be assumed, between the frequency of the impurity mode and that of the $\mathbf{q}=0$ TO phonon in the pure crystal.

The third step is to define an average complex dielectric constant, for the coupled oscillators $i = 1, 2$ in the ternary solid solution, as:

$$\varepsilon(\omega, x) = x \cdot \varepsilon_1(x, \omega) + (1 - x) \cdot \varepsilon_2(x, \omega) \quad (3)$$

where

$$\varepsilon_i(\omega, x) = \varepsilon_{i\infty} \left(1 + \frac{\Omega_i^2}{\omega_{T_i}^2(x) - \omega^2 - i\omega \cdot \gamma_i} \right) \quad (4)$$

$\Omega_1^2 = \omega_{L1}^2(1) - \omega_{T1}^2(1)$ and $\Omega_2^2 = \omega_{L2}^2(0) - \omega_{T2}^2(0)$ are related to the LO-TO splitting of the oscillators in their corresponding pure crystals. Hence the invariable effective charge of each oscillator in the ternary solution was assumed to be invariable. In the expression of $\varepsilon(\omega, x)$, we introduce empirical damping constants γ_i of oscillators.

It is known, from the Hon and Faust theory [8] for two oscillators coupled by the macroscopic electric field, that $\text{Im}(-\varepsilon^{-1})$ gives the expected contribution of the LO phonons to the Raman spectra. So the last step is to calculate this function for $0 < x < 1$. The calculated frequencies of $A_1(\text{LO})$ phonons are compared with the experimental values in Figure 4a. Peak values of the calculated function $\text{Im}(-\varepsilon^{-1})$, corresponding to the expected intensity of LO phonon lines, are plotted in Figure 4b.

5. Comparison of the calculated results with the experimental data

Good agreement is observed between the frequency measured for the LO phonon (A_1 or E_1) and the calculated LO branch corresponding to the AlN-like oscillator. The other LO branch corresponds to the weak structure, which is hardly evidenced in the $620\text{--}640\text{ cm}^{-1}$ range for solid solutions with low aluminium content. These experimental observations are completely explained by the very low intensity of the LO phonon for the GaN-like oscillator, compared to the AlN-like oscillator, as calculated by our model and illustrated in Figure 3b. So the so-called one-mode behaviour is found for the LO phonons in $\text{Ga}_x\text{Al}_{1-x}\text{N}$. It was previously interpreted in the case of zincblende III-V ternary solid solutions as a two mode-behaviour, with a quasi complete intensity transfer from one oscillator to the other [7].

6. Summary

The frequencies of long wavelength optical phonons of $\text{Ga}_{1-x}\text{Al}_x\text{N}$ solid solutions have been measured by Raman spectroscopy in the whole compositional range. These data give evidence for a one-mode behaviour of the A_1 and E_1 modes. The frequencies of the LO phonons were calculated from a model based on a dielectric formalism and were compared to the experimental results. Finally, a Fano interference effect observed in the Raman spectra is discussed.

References

- [1] K. Hayashi, K. Itoh, N. Sawaki, I. Akasaki, *Sol. St. Comm.* **77**, 115 (1991).
- [2] S. Clur, O. Briot, J. L. Rouvière, A. Andenet, Y-M. Le Vaillant, B. Gil, R. L. Aulombard, J. F. Demangeot, J. Frandon, M. Renucci, unpublished (1997).
- [3] LE Mcneil, M Grimsditch, RH French, *J. Am. Ceram. Soc.* **76**, 1132-1136 (1993).
- [4] K Karch, G Portisch, F Bechstedt, P Pavone, D Strauch, *Inst. Phys. Conf. Ser.* **142**, 967 (1996).
- [5] T. AZUHATA, T. MATSUNAGA, K. SHIMADA, K. YOSHIDA, T. SOTA, K. SUZUKI, S. NAKAMURA, *Physica B* **219-220**, 493 (1996).
- [6] J. GROENEN, R. CARLES, G. LANDA, C. GUERRET, C. FONTAINE and M. GENDRY, unpublished.
- [7] G. LANDA, R. CARLES and J.B. RENUCCI, "Local Bonding and Long-Range Order: Raman Investigation in III-V Solid Solutions», in *Proc. 18th Int. Conf. on Physics of Semiconductors, vol.2*, Ed. by O. Engström, (World Scientific, Singapore, 1987), p. 1361
- [8] D. T. HON, W. L. FAUST, *J. Appl. Phys.* **1**, 241 (1973).

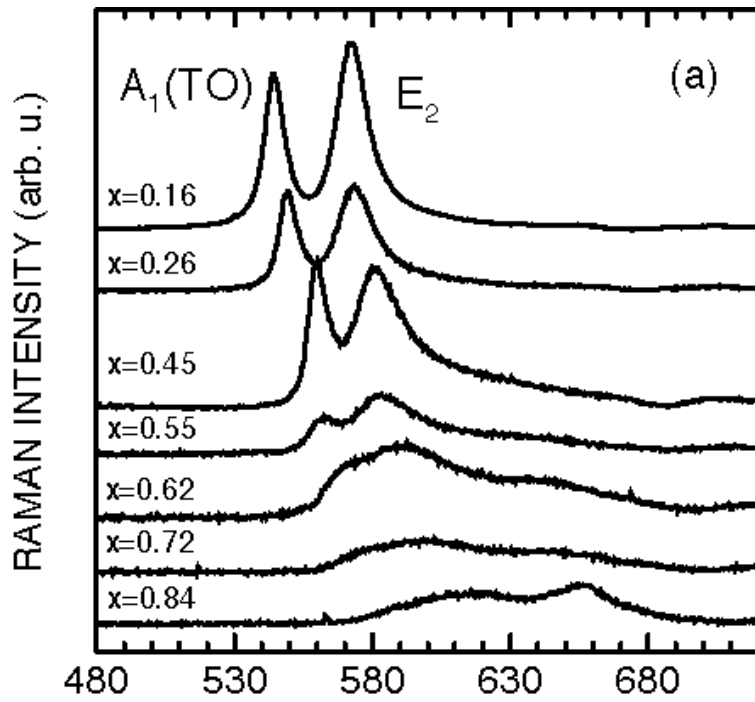
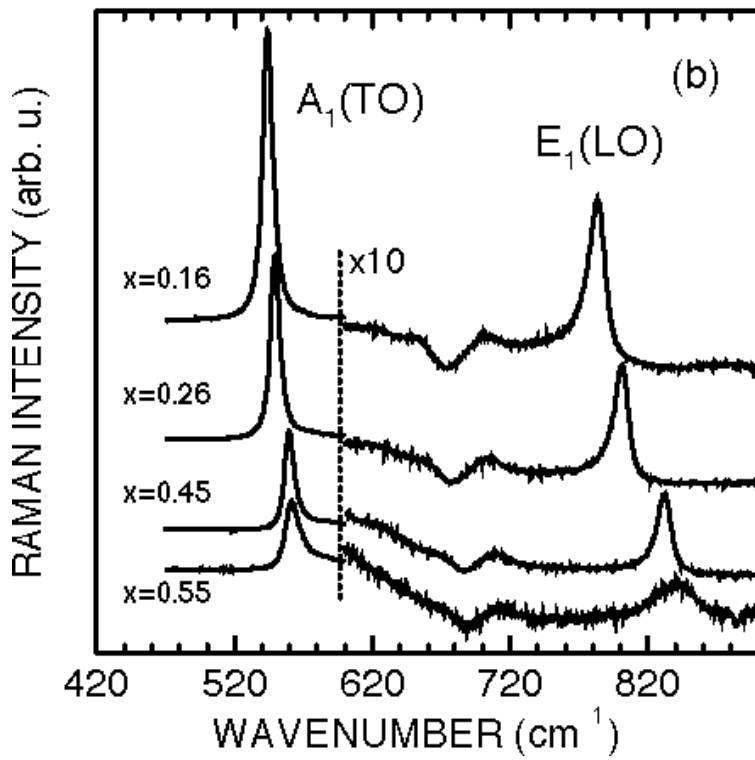


Figure 1. Raman spectra of $\text{Ga}_{1-x}\text{Al}_x\text{N}$ alloys recorded (a) in $x'(y'y')\bar{x}'$ configuration, (b) in $x'(\mathbf{z}\bar{z})\bar{x}'$ configuration.



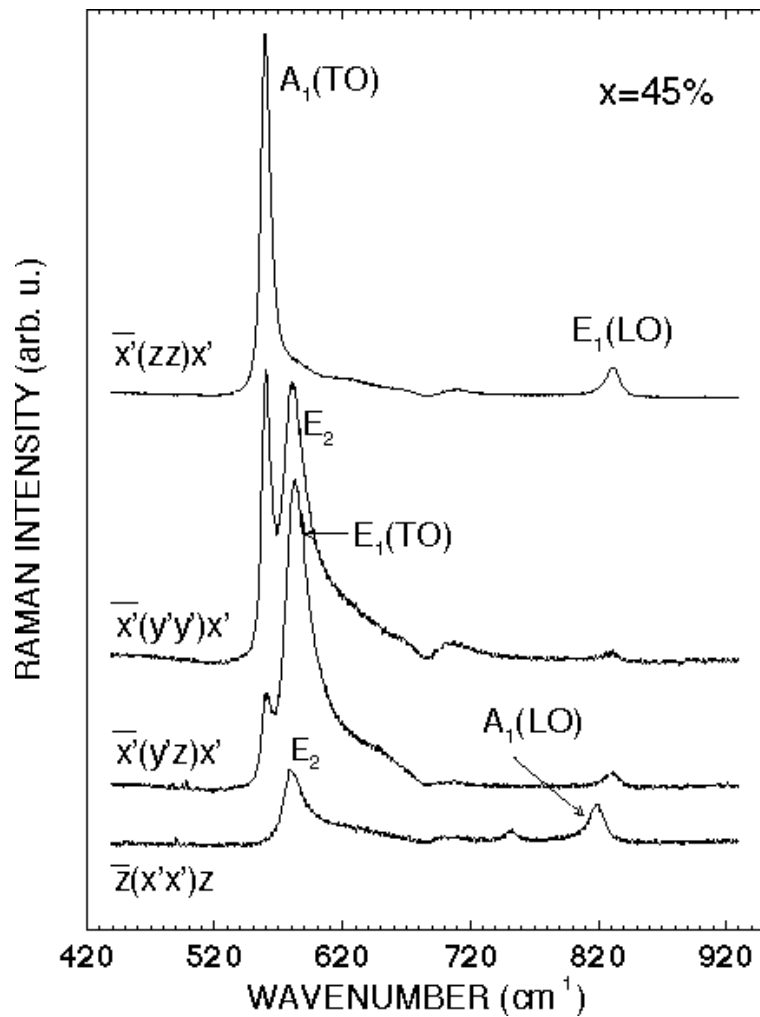


Figure 2. Check of the selection rules of Raman scattering, in the case of the $\text{Ga}_{0.55}\text{Al}_{0.45}\text{N}$ solid solution.

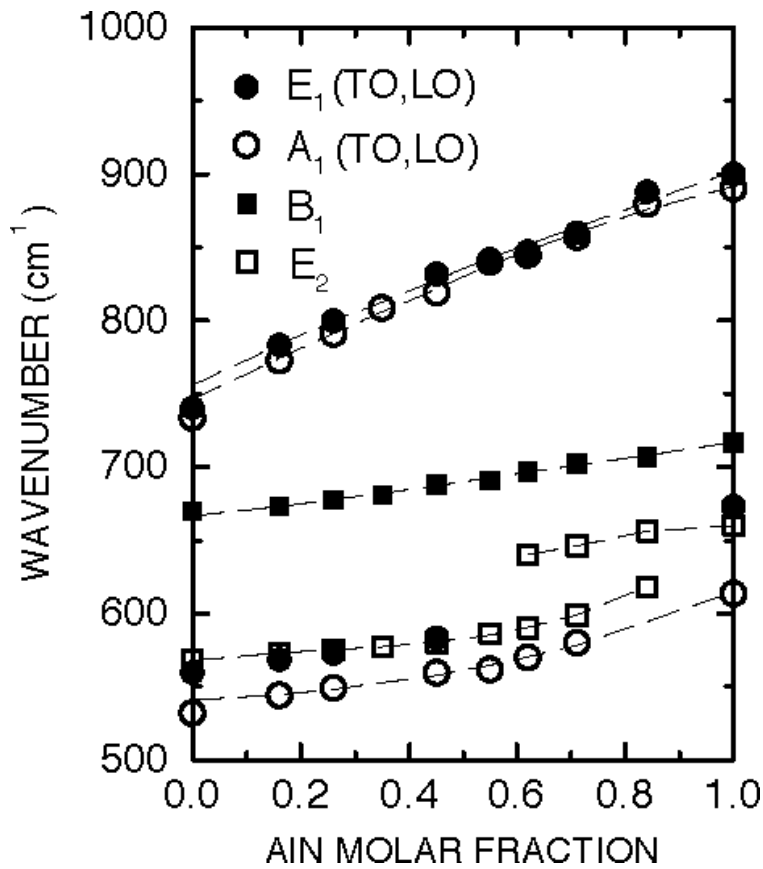


Figure 3. Variation of measured phonon for Ga_{1-x}Al_xN alloys. The so-called B₁ experimental points correspond to the dip observed in the spectra and discussed later.

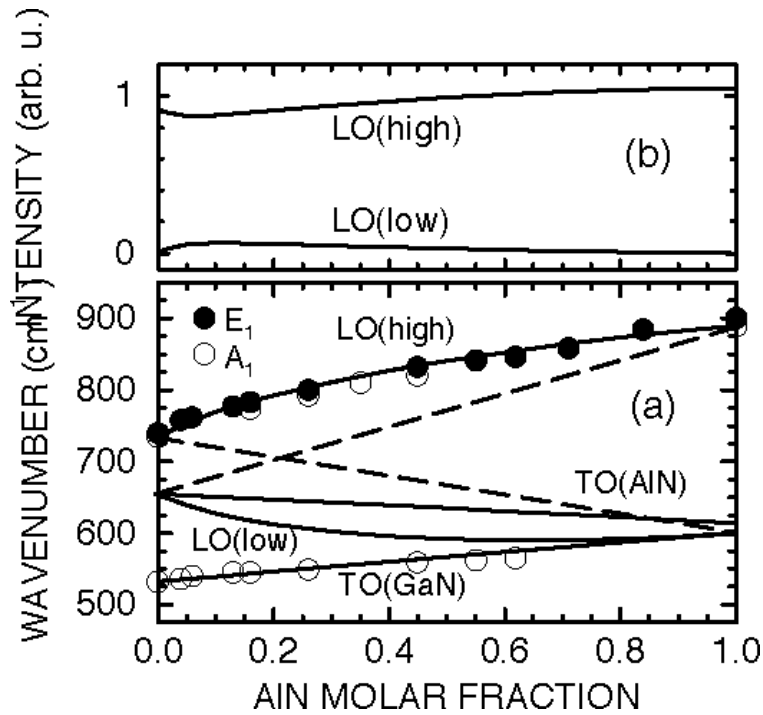


Figure 4. (a) Calculated and experimental frequencies of polar A₁ phonons; (b) Calculated intensity of AlN-like and GaN-like LO phonons.